Energy-Preserving Arbitrary Repetition-Rate Control of Periodic Pulse Trains Using Temporal Talbot Effects

Reza Maram, Luis Romero Cortés, James Van Howe, and José Azaña

(Invited Paper)

***Abstract*—The temporal Talbot effect comprises a set of self-imaging phenomena in which a pulse train undergoes various coherence revivals after propagation through a dispersive medium. Besides the intrinsic physical interest of the phenomenon itself, the effect has found practical applications in various scientific areas. In optical signal processing, the temporal Talbot effect has been used to multiply the repetition-rate of periodic pulse sequences by integer factors. Because it operates coherently on the frequencies that comprise a pulse train, the temporal Talbot effect has been shown to mitigate noise such as reduction of pulse-to-pulse timing jitter and amplitude variation, as well as real-time optical averaging. Recently, there has been renewed interest in the temporal Talbot effect due to its use in *arbitrary* repetition rate multiplication and division, not just *integer* multiplication. Arbitrary repetition-rate control is based on a suitable combination of temporal phase-modulation and spectral-phase filtering using temporal Talbot conditions. By adjusting the phase-modulation profile and group-velocity dispersion, the multiplication and division factors can be tuned to be any desired values- fractional or integer. One of the main advantages of this methodology compared to traditional approaches of repetition rate control is its energy efficiency. Because temporal and spectral phase filtering are lossless processes, pulse trains using Talbot-based repetition rate control only suffer insertion loss from the system. In this article, we first present an overview of the theory behind temporal Talbot effects and then review recent work on its application for realizing arbitrary control of the repetition-rate of periodic optical pulses. This platform enables the creation of simple, versatile optical pulse sources for diverse applications where customized repetition rates are necessary.**

***Index Terms*—Optical fiber communication, optical pulse generation, pulse repetition-rate division, pulse repetition-rate multiplication, temporal phase modulation, temporal Talbot effect, ultrafast optics.**

Manuscript received September 5, 2016; revised December 20, 2016; accepted December 29, 2016. Date of publication January 8, 2017; date of current version February 22, 2017. This work was supported in part by the Natural Sciences and Engineering Research Council of Canada, and in part by the Fonds de Recherche du Québec sur la Nature et des Technologies.

R. Maram, L. R. Cortés, and J. Azaña are with the Institut National de la Recherche Scientifique—Énergie, Matériaux et Télécommunications, Montreal, QC H5A 1K6, Canada (e-mail: r.maram.q@emt.inrs.ca; romero@emt.inrs.ca; azana@emt.inrs.ca).

J. V. Howe was with the Institut National de la Recherche Scientifique—Énergie, Matériaux et Télécommunications. He is now with the Department of Physics and Astronomy, Augustana College, Rock Island, IL 61201 USA (e-mail: jamesvanhowe@augustana.edu).

Color versions of one or more of the figures in this paper are available online at http://ieeexplore.ieee.org.

Digital Object Identifier 10.1109/JLT.2017.2648511

I. Introduction

TECHNIQUES for the generation, control and manipulation of periodic optical pulse trains, with repetition-rates in the sub-gigahertz, gigahertz and beyond, have become increasingly important for many scientific areas, including fiber optic communications, materials processing, frequency comb generation, nonlinear optics, photonic signal processing, optical sampling, and microwave/millimeter-wave photonics [1]–[9]. This has motivated extensive research on the development of new techniques for generating and controlling optical pulse sequences. Passive or active mode-locking is one of the main techniques for the generation of such optical pulses [10]–[16]. In active mode-locking, a cavity parameter is modulated electronically to force the laser to operate at the desired frequency [10]–[13]. Therefore, active sources are ultimately limited by the bandwidth of the electronics involved in the mode-locking process. Additionally, even though commercial active mode-locked lasers are presently available in the repetition-rate frequency between 5–42 GHz, it is difficult to achieve stable operation over a continuous range within this set of frequencies [10], [17], [18]. Passive mode-locking techniques [14]–[16], on the other hand, provide much more stable operation and offer the potential to overcome the limitations of active methods, as they are not limited by electronic bandwidths. However, they typically require a precise control of the optical properties of the laser cavity and offer very limited flexibility to program or tune the output repetition-rate.

A simple, cost-effective solution for arbitrary repetition-rate control, at repetition-rates beyond those practically achievable by conventional mode-locking, is to control the repetition-rate of a fixed and stable optical source outside the laser cavity, without having to modify the laser itself. To *arbitrarily* control the repetition-rate of an optical pulse source, one needs to be able to multiply and divide the original repetition-rate by any integer and fractional factors, leading to an output train of pulses with the desired repetition-rate, as shown in Fig. 1. This technique is often also useful for optical systems where various synchronized circuits are running at different repetition-rates, one circuit at the rate of the laser source (reference rate), and other periphery circuits at higher or lower rates [19]. To date, various rate multiplication and division techniques have been developed for

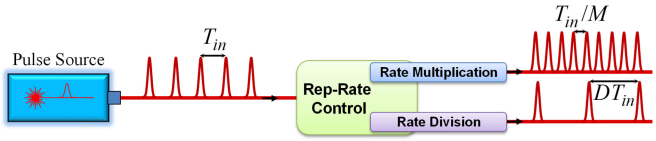

Fig. 1. Repetition-rate control of a fixed pulse laser through rate multiplication and division processes. M and D are multiplication and division factors, respectively.

converting the repetition rates of pulse trains outside of the laser cavity or independently of the laser source [20]–[32].

Repetition-rate division has been traditionally achieved by means of a temporally pulse-picking process using intensity modulators [20], to reduce the repetition-rate by a desired integer factor. Through this methodology, large amount of input energy is lost to obtain the target reduced repetition-rate pulses: losses scale up with the repetition-rate division factor.

On the other hand, ***repetition-rate multiplication*** is most often implemented by one of two methods of linear optical filtering: 1) spectral amplitude filtering [21]–[27] or 2) spectral phase-only filtering [28]–[32]. The amplitude filtering method consists of selecting specific spectral components of the input source, and eliminating the others, resulting in a repetition-rate increase. The periodic frequency separation of the selected spectral components corresponds to the output repetition-rate. Amplitude filters can be realized by using Fabry-Perot etalons [21], array waveguide gratings [22], [23], or superimposed fiber Bragg gratings (FBGs) [24]. One of the main drawbacks of this method is that it is very sensitive to a possible misalignment or a drift of the input source spectrum relative to the filter, especially for filters having high spectral selectivity/finesse. Moreover, the finite extinction ratio of the filtered components leads to a periodic amplitude modulation of the multiplied pulses. More importantly, a large amount of energy is lost during the filtering process, especially for higher rate multiplications.

On the contrary, rate multiplication techniques based on spectral phase filtering requires equal passing of all frequency components in amplitude, so that ideally no input energy is lost in the process. Typical methods for repetition-rate multiplication using spectral phase are based on the 'temporal Talbot effect' [26]–[32]. In addition to energy efficiency, Talbot-based rate multiplication techniques exhibit a simple configuration involving only a piece of a dispersive medium, such as an optical fiber. They are also robust against possible misalignments or drifts of the input source spectrum, and they have the capability of mitigating amplitude and phase noise present in the input pulse train- a capability that is intrinsic to the use of dispersion [33].

In all traditional techniques for repetition rate division and multiplication, the ratio of the output to the input repetition rate is constrained to be an integer. In addition, reconfigurability of the rate-multiplication factor is not possible without significant changes in the system configuration. Moreover, the physical mechanisms for multiplication and division are entirely different such that "arbitrary repetition rate control" is not possible using a single device, but requires the stacking of different systems.

Recently, we have developed a single platform using the temporal Talbot effect for arbitrary repetition rate control,

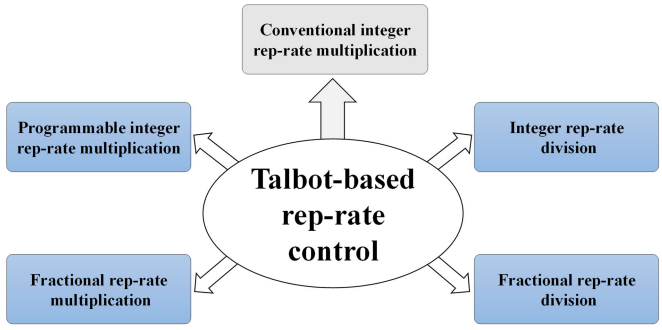

Fig. 2 Recent advances in repetition-rate control of periodic optical pulse trains based on temporal Talbot effects.

providing the possibility of not just multiplying the repetition rate by any fractional factors other than integers, but also dividing the original repetition rate by any fractional and integer factors. Additionally, this new platform provides a substrate to build a programmable integer repetition-rate multiplier. These advances are noted in Fig. 2 [34]–[38]. The proposed platform involves the use of a suitable combination of temporal phase modulation and dispersion-induced temporal Talbot effect on the input periodic pulse train. Arbitrary control of the repetition rate (involving repetition-rate multiplication and division by any integer and fractional factors) can be achieved by adjusting the phase-modulation profile and group-velocity dispersion value of the dispersive medium.

In this article, our goal is to provide a compact overview of the fundamentals of the temporal Talbot effect and then review the recent progress to date on the design, development and experimental demonstration of such methodology for arbitrary control of the repetition-rate of periodic optical pulses. In our review, we will narrow our attention to dispersion-induced temporal Talbot effects.

II. Temporal Talbot Effects

Temporal Talbot effects, also referred to as temporal self-imaging, are observed when a periodic temporal signal propagates through a first-order dispersive medium [29]. The dispersive medium is characterized by a linear group delay (quadratic phase response) as a function of frequency with a slope of ϕ_2, also referred to as the first-order dispersion coefficient. In the case of narrowband signal propagation through a single-mode optical fiber, the first-order dispersion coefficient, ϕ_2, also increases linearly with the propagation distance, $\phi_2 = \beta_2\, z$, where z is propagation distance and β_2 is the fiber dispersion parameter.

Fig. 3 shows the effect of first-order dispersion on the frequency components of a single optical pulse, versus a periodic pulse train, for different amounts of dispersion. Here, we show the joint time-frequency (TF) representation, similar to a spectrogram, to track the evolution of the spectral components of the pulse/pulse train as a function of time. For each TF representation, the bottom plot represents the temporal variation of the optical waveform and the plot at the left represents the corresponding spectrum, with the 2-D TF energy distribution shown

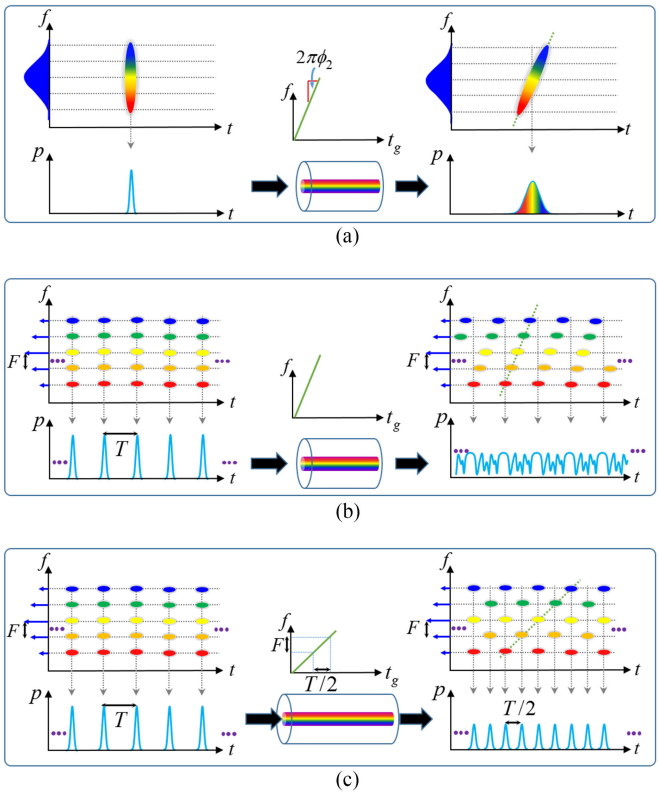

Fig. 3. Time-frequency analysis of linear propagation of optical waveforms in a first-order dispersive medium. t: time; f: frequency; p: instantaneous power.

in the larger, central plot. This 2D image provides information about the temporal location of the signal spectral components or in other words, it shows which of the spectral components of the signal occur at each instant of time. Fig 3(a) shows propagation of a short optical pulse exhibiting a wide spectrum. The spectral components of the pulse travel at different speeds, temporally shifting according to the group delay curve of the dispersive medium, i.e., a linear group-delay variation for first-order dispersion. More specifically, the pulse spectral components separate temporally from each other as they propagate through the dispersive medium, leading to the distortion and broadening of the temporal shape of the pulse.

An interesting situation occurs when a stream of flat-phase short optical pulses, repeating with temporal period of T (having discrete frequency components with spectral period of $F = 1/T$), propagates through a dispersive medium instead. As can be observed in Fig. 3(b), each individual pulse in the sequence contains the entire signal's spectral components, which occur in fact with an exact temporal synchronization. As expected for a dispersive process, the individual pulses are first temporally broadened, see Fig. 3(a). As the signal continues propagating through the dispersive medium, the neighboring pulses start to overlap temporally giving rise to inter-pulse interference and distortion of the individual input pulses.

However, if we choose the dispersion value according to a temporal Talbot effect condition (specific equations defined below), the inter-pulse interference leads to a reproduction of the original pulse shape (self-image of the original signal), either with the same temporal period or a smaller temporal period than that at the input, Fig. 3(c). In the particular example shown here, the dispersion value is fixed such that discrete spectral components spaced by a frequency period of F are delayed with respect to each other by half the original pulse rate period ($T/2$). As a result, we observe the formation of individual pulses occurring with period two times shorter than that at the input and where the corresponding frequency bands are vertically realigned (resynchronized).

In fact, the Talbot condition, Eq. (2), predicts an infinite amount (though discrete) of such locations along the dispersive medium where frequency components realign and resynchronize, in a similar way to that illustrated for the 2-times rate multiplication process in Fig. 3(c). Therefore, as the optical pulse train propagates further along the dispersive medium, we will observe many self-images of the original signal. A map of these coherence revivals as they occur for increasing dispersion resembles an ornate Persian rug and has been named the "Talbot Carpet." Fig. 4 shows a small portion of the Talbot Carpet.

In particular, Fig. 4 represents the evolution of a flat-phase input pulse train through a section of a dispersive optical fiber. The input pulse train (at $z = 0$) is perfectly self-imaged after dispersive propagation through an integer multiple of the fundamental Talbot distance, z_T, (integer Talbot images) defined as [29]:

$$\phi_2 = \beta_2 z_T = \frac{T_{\text{in}}^2}{2\pi} \tag{1}$$

where T_{in} is the repetition period of the input pulse train at $z = 0$.

Moreover, in addition to the mentioned 'integer' self-images, there also exists an infinite amount of fractional distances (fractional values of the fundamental Talbot distance) where rate-multiplied self-images of the original input pulse train are obtained at [29]:

$$\phi_2 = \frac{s}{m}\beta_2 z_T = \frac{s}{m}\frac{T_{\text{in}}^2}{2\pi} \tag{2}$$

where s is a positive integer and co-prime with $m\,(= 2, 3, 4, \ldots)$. In the conventional Talbot effect, the rate-multiplication factor is equal to m, $M = m$. See examples in Fig. 4 at the fractional Talbot distances $z_T/2$, $2z_T/3$, and $3z_T/4$. As mentioned above, dispersive propagation speeds up and slows down the different frequency-component "colors," originally in-phase that make up the pulse train, redistributing the original signal energy into the mentioned different temporal intensity patterns. An integer self-image exhibits the same repetition rate as the input, whereas in the multiplied self-images, the repetition rate is increased, and the individual pulse intensity is correspondingly decreased by an integer factor. In particular, the repetition-rate multiplication (and corresponding intensity division) factors for the multiplied self-images shown in Fig. 4 at $z_T/2$, $2z_T/3$, and $3z_T/4$ are integer numbers of 2, 3, and 4, respectively. We recall that the term self-image refers to the fact that the temporal shape of each individual waveform in the Talbot patterns is an exact, undistorted copy of the input.

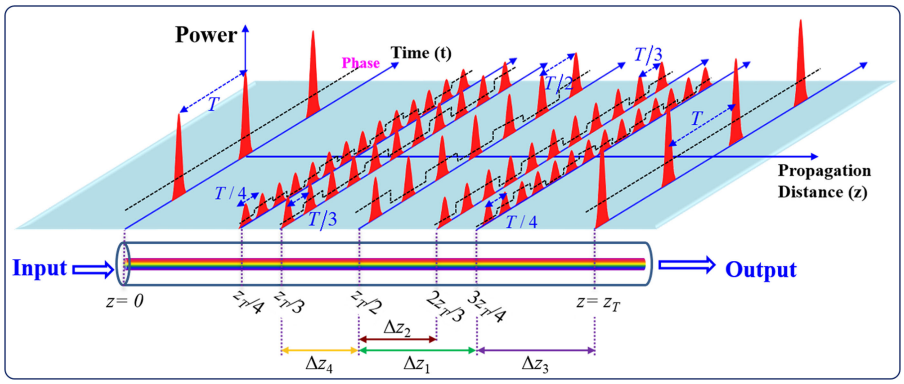

Fig. 4. Standard temporal Talbot effect. Evolution of the intensity and phase of a repetitive input pulse train through propagation along a first-order dispersive medium, where the group delay depends linearly on the frequency variable, also linearly increasing with the propagation distance (z). The multiplied self-images are affected by a deterministic pulse-to-pulse residual temporal phase profile (dashed black).

In addition to intensity, the temporal phase of the input pulse train also evolves as it propagates through the dispersive medium. In an integer self-image, the uniform temporal phase profile of the input is also restored. However, the multiplied self-images, such as those observed at distances $z_T/2$, $2z_T/3$, and $3z_T/4$ are affected by a deterministic pulse-to-pulse residual temporal phase structure (dashed black lines in Fig. 4). For instance, at the fractional distance $z_T/2$, in the case of multiplication by $m = 2$, the dispersive medium produces two replicas of the pulses with a repeating temporal phase profile of 0, $\pi/2$, 0, $\pi/2$, ... The residual phase for a particular fractional image can be analytically calculated for a given *s* and *m*. The phase function of the *n*-th pulse of a particular fractional image, φ_n, with a given *s* and *m* can be analytically obtained as [39], [40]:
when *s* is even and *m* is odd or *vice versa*,

$$\varphi_n = -\frac{s}{m}\left(\left[\frac{1}{s}\right]_m\right)^2 \pi\, n^2 \tag{3.a}$$

when both *s* and *m* are odd

$$\varphi_n = -2\frac{s}{m}\left[\frac{1}{2}\right]_m \left(\left[\frac{1}{2s}\right]_m\right)^2 \pi\ (2n+m)^2 \tag{3.b}$$

where $[\frac{1}{a}]_b$ is the inverse of a modulo b. If these phase shifts are reduced to a 2π range, a periodic sequence of phase steps with a fundamental period equal to *m*, namely $\varphi_n = \varphi_{n+m}$, is obtained; see examples in Fig. 4.

Most of the practical applications of the Talbot effect presented to date (i.e. before our proposed methodology) have concentrated on of the temporal distribution of the input signal's intensity and neglected the phase properties. However, in the following Section, we show how the phase properties yield a powerful tool to provide an unprecedented degree of flexibility to control and manipulate the output pulse repetition rate and corresponding energy per pulse.

III. Talbot-Based Rep-Rate Control

Despite its attractive set of advantages, traditional Talbot-based rate multiplication exhibits a number of intrinsic constraints that impair its practical use. For instance, as can be inferred from Eq. (2) and Fig. 4, the technique is limited only to multiply the repetition rate by an exact integer multiple of the input, i.e., the possibility of performing rate multiplication by fractional factors is not attainable. Moreover, such systems are not tunable. Multiplication factors are chosen by implementing a fixed amount of dispersion in order to impart a precise amount of spectral phase, typically through a section of dispersive fiber or a linearly chirped fiber Bragg grating (LC-FBG). It is therefore not straightforward to tune or program the rate-multiplication factor without changing the dispersive element-a significant system reconfiguration.

However, the self-imaging condition in Eq. (2) only applies to the conventional rate multiplication processes starting from $z = 0$, where the input signal is a flat-phase pulse train, to a multiplied image at a fractional distance. As can be inferred from Fig. 4, there exists another possible set of rate transformational processes on the Talbot carpet, i.e., the repetition-rate alters by moving from one self-image to the other. In order to overcome the aforementioned limitations of the temporal Talbot effect, one need only consider the unlimited possible rate transformational processes along the carpet. Essentially, by taking into account the temporal phase, one can gain access to the intermediate planes on the carpet and start *at any location* within the carpet (not necessarily at $z = 0$) so that to transform the input periodic waveform to that obtained at *any other desired location* in the carpet. Hence, accessing intermediate planes by controlling the temporal phase provides a versatile key to realize any desired rep-rate change.

For example, one can start from a multiplied image at a fractional distance as the input, and transform to the next appropriate fractional or integer distance. This transition on the carpet enables the possibility of both *repetition-rate multiplication and division with any fractional and integer factors*. As shown in Fig. 4, for example, a pulse train starting at a fractional distance $z_T/2$ will be rate multiplied by a factor of $M = 2$ at the fractional distance $3z_T/4$. Or the input pulse train starting at a fractional distance $z_T/2$ will be rate divided by a factor of $D = 2$ at the integer distance of z_T. To realize these repetition-rate multiplication and division processes, it requires first the application of a prescribed temporal phase-modulation profile to a flat-phase input signal to make it "appear" like the

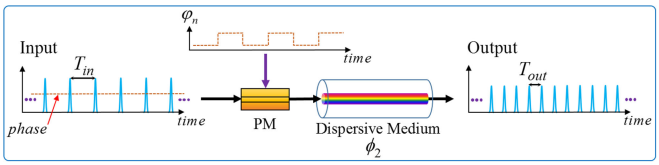

Fig. 5. Configuration of the proposed platform to control the repetition-rate of an optical pulse train with a temporal period of $T_{\rm in}$. $T_{\rm out}$ is the temporal period of output periodic pulses, and PM is a phase modulator.

pulse train at the starting fractional distance. Next, it requires propagation through an appropriate dispersive delay in order to reach the final target fractional/integer self-image. For instance, if we phase condition a flat-phase input pulse train, by phase modulation profile of 0, $\pi/2$, 0, $\pi/2$, ..., to look like the pulse train at $z_T/2$, subsequent propagation through $z_T/2$ more of dispersive propagation will give the output shown at z_T, one-half the repetition-rate. Fig. 5 illustrates the resulting designed platform for the repetition-rate control methodology, where the rate-multiplication or division factor is determined by the phase modulation function, φ_n, and dispersion ϕ_2.

Phase-modulation of the input pulses along the time domain can be performed either electro-optically [41], [42] or through an optical nonlinear process [43]–[45]. In this design, we choose the electro-optic phase modulation scheme as this offers the simplest and most energy-efficient (i.e., the lowest energy) mechanism for temporal modulation of an optical signal. A crucial advantage to this new platform for repetition rate control is that it involves two lossless processes- temporal phase modulation and spectral phase filtering. The output signal energy is only reduced by the insertion loss of the phase filtering devices, preserving nearly all of the input signal energy.

In this Section, we will show how if the temporal phase modulation function $\varphi_{\rm n}$, and spectral phase modulation ϕ_2, are properly selected, a variety of repetition-rate controlling processes can be implemented. Our discussion is organized as follows: (III.A) Energy-preserving programmable integer rep-rate multiplication using a fixed dispersion, (III.B) Energy-preserving fractional repetition-rate multiplication of optical pulse trains, (III.C) Energy-preserving integer repetition rate division of optical pulse trains, and (III.D) Energy-preserving fractional repetition rate division of optical pulse trains.

A. *Programmable Integer Rep-Rate Multiplication*

As mentioned above, a Talbot-based rate multiplier requires the use of a proper, fixed amount dispersion (e.g., a length of dispersive fiber or a LC-FBG) for a given integer multiplication factor [29]. For a given input signal with a repetition period of $T_{\rm in}$, the amount of dispersion is strongly dependent on the multiplication factor, $M = m$, Eq. (2). Hence, in order to modify the multiplication factor in this technique, one needs to change the dispersive medium accordingly. This has been the primary impediment to realizing a tunable multiplication technique based on dispersion-induced Talbot effect, owing to the fact that available dispersive media (e.g., optical fibers or LC-FBGs) do not possess the flexibility to modify their group delay dispersion without mechanical manipulation. To overcome this constraint, one can exploit alternative integer-rate multiplication processes also observed along the Talbot carpet. For example, a multiplied self-image at the fractional distance $z_T/2$ will be multiplied in repetition-rate by a factor of $M = 2$ at the fractional distance $3z_T/4$. As a matter of fact, in this design, the self-image at $z_T/2$ plays the role of the input pulse train, with a repetition period of $T_{\rm in}$, and the self-image at $3z_T/4$ is the output with a temporal period of $T_{\rm out} = T_{\rm in}/M$. This process can be emulated using the scheme in Fig. 5, pre-introduction of the temporal phase of the self-image signal at $z_T/2$ to a flat-phase input signal by means of a phase-modulation mechanism and propagation through an appropriate amount of dispersion. The needed amount of dispersion for this rate multiplication process is the difference between the fractional distance $z_T/2$ and the fractional distance $3z_T/4$, i.e. Δz_1 in Fig. 4. Mathematical calculations presented in [34] show that, if the two fractional self-images are properly selected, the amount of dispersion between these two fractional self-images is independent of the desired rate-multiplication factor, *M*, depending only on the temporal period of the input pulse train to be processed. The derived analytical expression for the required dispersion of the dispersive medium is [34]

$$\phi_2 = \beta_2 \Delta z_1 = \frac{T_{\rm in}^2}{2\pi} \tag{4}$$

Note that Eq. (4) only involves the repetition period of the multiplied image at the starting fractional distance, i.e. $T_{\rm in}$, and does not depend on the desired rate multiplication factor "*M*". This condition is indeed analogous to that of the conventional integer self-imaging shown in Eq. (1), nevertheless, it applies for all multiplication factors. For example, as mentioned above, though the multiplication factor is $M = 2$ for the multiplication process from the fractional distance $z_T/2$, to the fractional distance $3z_T/4$, the differential dispersion is as shown in Eq. (4). This is the main consequence of Eq. (4), implying that for a given input signal, unlike the condition in Eq. (2), the required dispersion is fixed for all multiplication factors ($M = 1, 2, 3, 4, \ldots$).

The required temporal phase modulation profile to be applied on the input optical pulse train is obviously the pulse-to-pulse phase profile corresponding to the fractional self-image at the starting fractional distance, to be calculated by Eq. (3) (for rate multiplication by a factor *M*).

For a given multiplication factor, *M*, we only need to apply the corresponding phase function in Eq. (3) on the *n*-th incoming temporal pulse ($n = 0, 1, 2, \ldots, m-1$, and periodically repeated). Note that in Eq. (3), for a given *m*, *s* can be chosen arbitrarily as long as it is a co-prime with *m*. By setting $s = m - 1$, we can simplify further the required phase functions in Eq. (3). The resultant phase modulation function then can be re-written as [34]:

$$\varphi_n = \frac{m-1}{m}\pi n^2 \tag{5}$$

Hereafter, we name *m* as the phase modulation parameter. In this programmable rate multiplier design, the multiplication factor is equal to the phase modulation parameter, i.e., $M = m$. Note that the phase shift in Eq. (5) has been shown to induce a

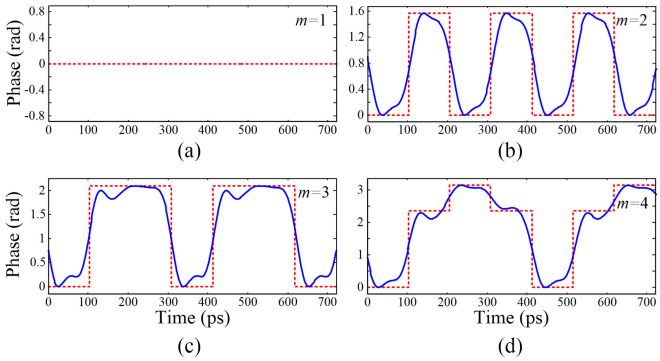

Fig. 6. Temporal phase-modulation patterns required for multiplication factors $M = m = 1, 2, 3$, and 4, as determined by Eq. (4). The dashed red lines show the ideal temporal phase profiles, and the solid blue lines show the actual phase drive delivered by the AWG.

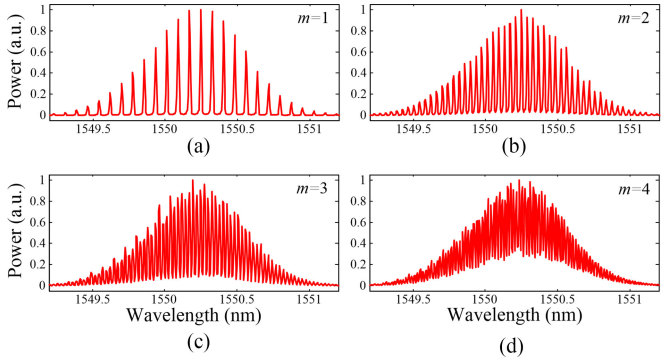

Fig. 7. Measured optical spectra of the optical pulse trains after phase modulation.

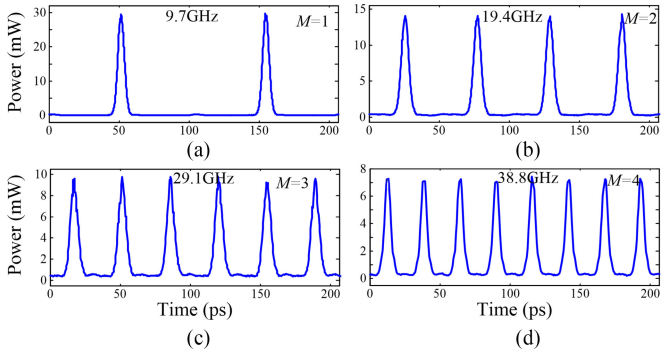

Fig. 8. Optical sampling oscilloscope (OSO) time trace of pulse trains at the dispersive fiber output for the desired multiplication factors of $M = m = 1, 2, 3$ and 4.

spectral self-imaging effect on the modulated pulse train [41], [42]. In particular, the temporal phase-modulation process produces new frequency components, reducing the frequency spacing of the input signal discrete comb-like spectrum by an integer factor of m.

In summary, if the value of the dispersive medium in Fig. 5 is fixed to satisfy the condition Eq. (4) with the repetition period of T_{in}, the repetition-rate of the output signal can be programmed simply by modifying the temporal phase-modulation function obtained from Eq. (5) for any given integer m. Notice that when $m = 1$, the phase function Eq. (5) is constant and equal to zero, i.e., $\varphi_n = 0$. This case corresponds to the conventional integer Talbot effect where the input signal is exactly replicated at the output.

We experimentally have demonstrated tunable repetition-rate multiplication by factors ranging from $M = 1$ to 4 of a 9.7 GHz mode-locked fiber laser source, generating phase-coherent, nearly transform-limited Gaussian-like pulses with a FWHM of 6-ps at 1550 nm. The input optical pulse train is first phase-modulated in the time-domain by a 25 GHz bandwidth commercial electro-optic PM (EOspace), driven by an arbitrary waveform generator (AWG) (Tektronix AWG7122C, 7.5 GHz analogue bandwidth). The pulses are then propagated through a dispersion-compensating fiber (DCF) module, providing a fixed first-order dispersion coefficient of $\phi_2 \approx 1690\,\text{ps}^2/\text{rad}$.

Fig. 6 shows the prescribed electro-optic phase modulation profiles (φ_n), derived from Eq. (5), applied to the input optical pulses, for the cases when we target multiplication factors from $M = m = 1$ to 4, respectively. The temporal phase functions are generated from the AWG. The dashed red lines show the ideal temporal phase profiles uploaded in the AWG, and the blue solid lines show the actual phase drive delivered by the AWG captured with a 40-GHz electronic sampling oscilloscope (ESO) in the averaging mode with 16 averages.

Fig. 7 shows the optical spectra of the signals after temporal phase modulation, recorded with an optical spectrum analyzer, showing the predicted spectral self-imaging effect, leading to the anticipated reduction in the comb frequency spacing of the input signal by factors of $m = 1, 2, 3$ and 4, respectively. Fig. 8 shows the temporal intensity waveforms of the resultant multiplied pulse trains after dispersion. All the optical temporal waveforms throughout this paper were measured by a 500-GHz bandwidth optical sampling oscilloscope (OSO) in the averaging mode with 4 averages, unless otherwise specified. The multiplied rates after dispersion are 9.7, 19.4, 29.1 and 38.8 GHz, confirming the functionality of the proposed tunable pulse rate multiplication scheme. The deterioration on the pedestal of each output pulse train is likely inherited from the presence of low-power pedestals at the input signal.

B. Fractional Rep-Rate Multiplication

All the demonstrated repetition-rate multiplication techniques, including those based on Talbot effects, are limited to output repetition-rates that are "integer" multiples of the initial pulse repetition rate. Therefore, for example, using a fixed 10 GHz pulse source, it is not attainable to produce a needed 15 GHz train of pulses.

Here we show how the same scheme shown in Fig. 5 can also be reconfigured to achieve any desired fractional repetition rate multiplication factor [35]. As a matter of fact, rate multiplication processes on the Talbot carpet, from a multiplied self-image to a next one with a higher rate, are not necessarily limited to integer rate-multiplication factors. As shown in Fig. 4, repetition rate of a pulse train starting at the fractional distance $z_T/2$ will be multiplied by a fractional factor of $M = 3/2 = 1.5$ at the fractional distance $2z_T/3$. Likewise, a pulse train starting at the

fractional distance $2z_T/3$ will be repetition-rate multiplied by fractional factor of $M = 4/3 = 1.33$ at the fractional distance $3z_T/4$. According to the Talbot carpet, any desired fractional repetition-rate multiplication factor can be obtained, as long as the output period is sufficiently long so that individual pulse waveforms do not overlap along the time domain. Generally, the rate-multiplication factor can be designed to be any desired fractional number, expressed as $M = q/m$, where *m* and *q* are two co-prime integers and $q > m$. In fact, *m* is the multiplication factor of the starting multiplied image and *q* is the multiplication factor of the target multiplied image, with respect to the flat-phase pulse train at $z = 0$, see in Fig. 4. Therefore, similar to the programmable rate multiplier design, in Fig. 5, we use the phase profile function of the starting self-image, that is the same phase profile function introduced in Eq. (5). Recall that we named *m* as the phase modulation parameter. In this case, for example, for a phase modulation parameter of $m = 2$, the multiplication factor will be $M = q/m = q/2 = 1.5, 2.5, 3.5, \ldots$ (for $q = 3, 5, 7, \ldots$, respectively) or for a phase modulation parameter of $m = 3$, the multiplication factor would be $M = q/m = q/3 = 1.33, 1.66, 2.33, 2.66, 3.33 \ldots$(for $q = 4, 5, 7, 8, 10, \ldots$, respectively). However, the amount of the required dispersive medium is different than that of the programmable rate multiplier and can be calculated by the differential distance between the selected multiplied fractional distances, e.g., Δz_2 distance between $z_T/2$ and $2z_T/3$ in Fig. 4. Therefore, the dispersive medium should introduce a dispersion value of [35]:

$$\phi_2 = \beta_2 \Delta z_2 = \frac{1}{M}\frac{T_{\text{in}}^2}{2\pi}. \tag{6}$$

Notice that, unlike the programmable rate multiplier design, the needed amount of dispersion for the fractional rate multiplication is inversely proportional to the rate multiplication factor, *M*. Hence, in order to modify the fractional multiplication factor, one needs to change also the dispersive medium accordingly.

Fig. 9 represents experimental verification of this concept by demonstrating the fractional rate multiplication by factors of $M = q/m = 1.5, 2.5$ (where the denominator of *M* or phase modulation parameter is $m = 2$ and the numerators are $q = 3$, and 5, respectively) and $M = 1.33$ and 2.33 (where the denominator of *M* or phase modulation parameter is $m = 3$ and the numerators are $q = 4$, and 7, respectively). The original laser periodic pulses are first phase-modulated along the time domain by an electro-optic PM with a phase function obtained from Eq. (5) for phase-modulation parameters of $m = 2$ and 3. Subsequent propagation through a first-order dispersive medium, whose dispersion coefficient is fixed to satisfy the condition Eq. (6), $\phi_2 \approx 890\,\text{ps}^2/\text{rad}$, will provide the output pulse train with a repetition rate *M*-times that of the input sequence. The used phase modulation profiles $m = 2$ and 3 are the same as Figs. 6(b) and (c), respectively.

C. Integer Rep-Rate Division

The temporal Talbot effect has been traditionally known as a phenomenon that is capable of multiplying the repetition-rate of periodic pulse sequences — the generation of higher repetition-rate pulses from a lower repetition-rate pulse train. In this multiplication process, the peak intensity of individual input pulses is reduced with the same multiplication factor. In [36], we performed a reverse-engineering of the conventional Talbot effect, that is referred to as the "inverse temporal Talbot effect", to develop an energy-preserving repetition-rate division technique,—the generation of lower repetition-rate pulses from a higher repetition-rate pulse train.

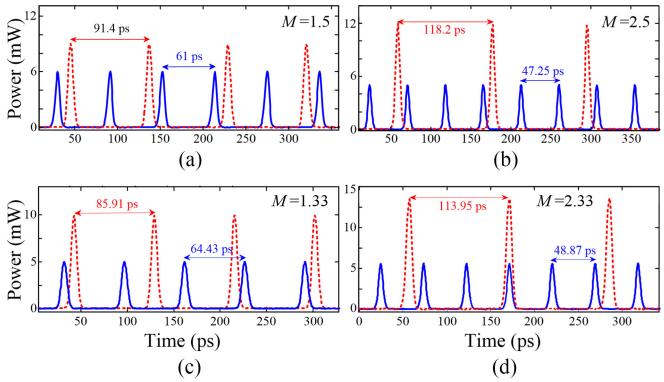

Fig. 9. Experimental results of fractional rate multiplication. (a)-(d) Measured temporal waveforms of the input pulse trains (dashed red) together with their self-imaged fractional rate-multiplied copies (solid blue). The repetition-rate of the input and output pulse trains, respectively, are (a) 10.9 GHz and 16.4 GHz ($= 10.9\,\text{GHz} \times 1.5$), (b) 8.46 GHz and 21.16 GHz ($= 8.46\,\text{GHz} \times 2.5$), (c) 11.64 GHz and 15.52 GHz ($= 11.64\,\text{GHz} \times 1.33$), (d) 8.77 GHz and 20.46 GHz ($= 8.77\,\text{GHz} \times 2.33$). Notice that for all represented traces (input and output pulse trains), the intensity profiles are plotted normalized with respect to the corresponding pulse peak power.

If we choose any multiplied image at a fractional distance on the Talbot carpet as the input, instead of the conventional phase-free input at $z = 0$, further dispersive propagation to the integer Talbot distance z_T produces an output with reduced repetition rate by integer factors, i.e., $D = 2, 3, 4, \ldots$. As shown in Fig. 4, the repetition-rate of a pulse train starting at the fractional distance $3z_T/4$ will be divided by a factor of $D = 4$ after a dispersive propagation of $\Delta z_3 = z_T/4$ to the integer Talbot distance z_T.

Using the same scheme in Fig. 5, we can emulate this repetition-rate division process. We first phase-modulate a flat-phase input to make it look like a pulse train at a fractional distance on the Talbot carpet. The phase modulation function can be obtained by Eq. (5) for a given phase-modulation parameter, *m*. The resulting pulse train after phase modulation is then propagated through a Δz_3 more of dispersion to reach the Talbot distance z_T. The amount of dispersion that is needed to move from a fractional self-image to the Talbot distance is [36]

$$\phi_2 = \beta_2 \Delta z_3 = m\frac{T_{\text{in}}^2}{2\pi} \tag{7}$$

In this problem, the division factor is equal to the phase modulation parameter, i.e., $D = m$. Note that the needed amount of dispersion for the integer rate division depends on the rate division factor, *D*. Hence, in order to modify the division factor, one needs to change also the dispersive medium accordingly.

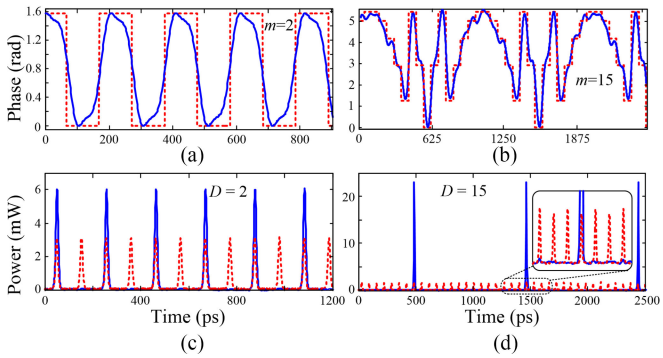

Fig. 10. Experimental results of repetition-rate division by integer factors. (a) Prescribed temporal phase modulation profiles; (b) Temporal trace of input (dashed red) and output (solid blue) showing repetition-rate division and corresponding pulse peak power amplification by the factors $D = 2$ and 15.

Since only phase manipulations are involved in the combined temporal phase-modulation and temporal Talbot process, the total energy of the original pulse train is preserved, aside from practical passive losses associated to the different optical components involved. Therefore, such a rate division process can be interpreted as coherently adding the input pulses' energy into fewer pulses (i.e., coherent addition of energy of every *D* pulses into one pulse), resulting in each output individual pulse to be an amplified copy of the input. This can be perceived in Fig. 4; for example, the peak power of individual pulses starting at the fractional distance $3z_T/4$ will be amplified by the same order as the rate division factor $D = 4$ at the integer Talbot distance z_T. In general, if the pulse peak power of the input train is P_{in} and the temporal period is T_{in}, the process transforms it into a train with a temporal period of $T_{\text{out}} = D \times T_{\text{in}}$ and with a pulse peak power equal to $P_{\text{out}} = D \times P_{\text{in}}$ [36].

Fig. 10 shows two examples of repetition rate division by the factors of $D = 2$ and 15 and corresponding pulse intensity amplification. Figs. 10(a) and (b) show the prescribed electro-optic phase modulation profiles prescribed by Eq. (5), φ_n, applied to input optical pulses, for the cases when we target rate division factors of $D = m = 2$, and 15. The experimental results of the demonstrated energy-preserving repetition-rate division with factors of $D = 2$, and 15 at the output of the following dispersive fiber module are illustrated in Fig. 10(c) and (d), demonstrating the predicted repetition-rate division and corresponding pulse intensity amplification processes. The system presents a passive power gain of *D*. The original repetition rates of the input pulse trains in the two reported experiments are 9.7 GHz, and 15.43 GHz, respectively. The reduced rates after the dispersion are 4.85 GHz, and 1.03 GH, respectively.

Notice that the discussed estimates on power gain and related results (shown in Fig. 10) do not consider passive insertion losses in the rate-division circuit. Due to large amounts of group delay required (1,000–10,000 ps/nm) for moderate division factors, dispersion spectral phase from optical fiber introduces impractical losses. However, dispersive losses can be reduced to below 1dB by instead using a suitably designed dispersive line such as a high-reflectivity LC-FBG [37]. This energy-preserving repetition-rate division process is also referred to as the Talbot amplification [36], [37]. Due to this amplification feature, we have shown in [36], [46], [47] how this rate division process produces an effective real-time averaging effect on the noise fluctuations of the individual repeating waveforms of the train. In particular, Fig. 11 shows how this process performs similarly to a conventional averaging process, e.g., scope averaging of *N* consecutive pulses, on amplified spontaneous emission (ASE)-like intensity noise fluctuations. Fig. 11(a) shows experimental data for the coefficient of variance (CV), the ratio of the standard deviation to the mean for the top level, of a noisy pulse (optical signal to noise ratio (OSNR) = 10) versus the inverse of the square root of amplification factor $D = N$ (red squares). Also shown is the CV versus the inverse of the square root of number of scope averages *N* (blue circles), demonstrating the equivalence of Talbot amplification to averaging. The theoretical trend line for scope averaging, which scales as *N*, is overlaid (dashed green). Experimental sampling oscilloscope traces in Figs. 11(b) and 11(c) show how the point-to-point fluctuation is nearly the same for Talbot amplification and scope averaging.

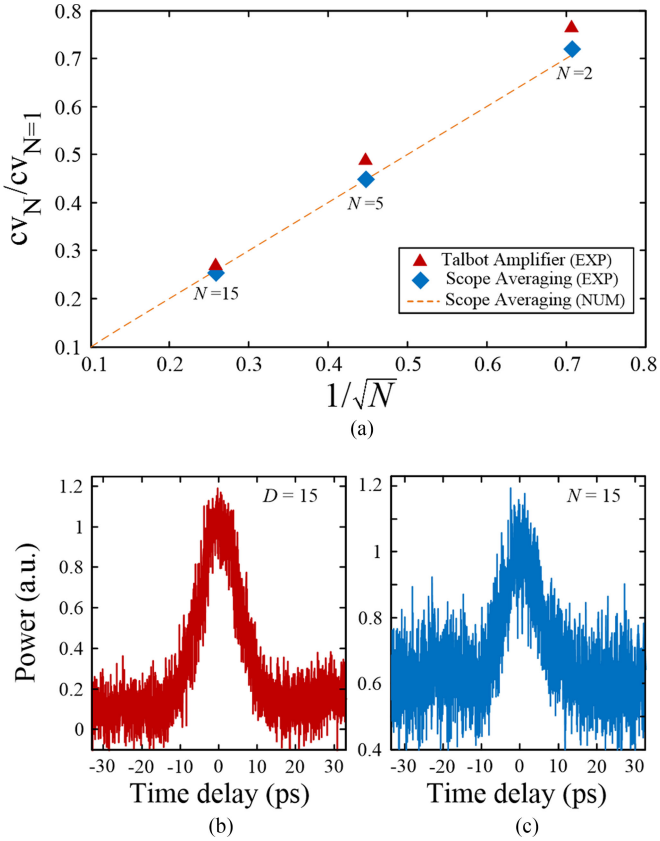

Fig. 11. Averaging effect of Talbot amplification for ASE-like noisy fluctuations. Ratio of pulse variance to mean versus $1/\sqrt{N}$, N = averages = m. (b) and (c) Electrical sampling oscilloscope traces (b) with passive amplification of $m = 15$ and no scope averaging, (c) without passive amplification and scope averages of $N = 15$, for OSNR = 10.

Fig. 11(b) shows results for a Talbot-amplified pulse by $D = 15$ with no scope averaging, and Fig. 11(c) shows results for a pulse without passive amplification and a regular scope average of $N = 15$. Passive amplification is therefore equivalent

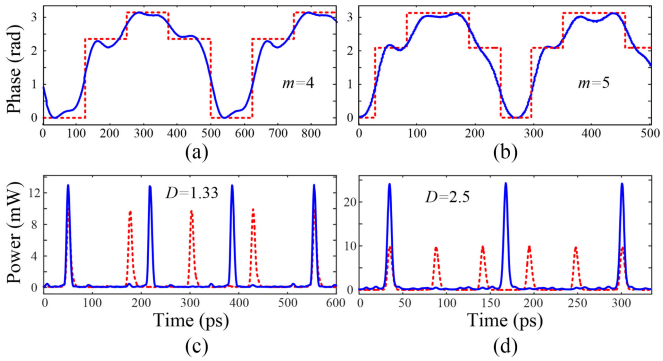

Fig. 12. Experimental results of repetition-rate division by fractional factors. (a) Prescribed temporal phase modulation profiles; (b) Temporal trace of input (dashed red) and output (solid blue) showing repetition-rate division and corresponding pulse peak power amplification by the factors $D = 1.33$ and 2.5.

to a real-time optical average. Said another way, Fig. 11(b) is the equivalent of Fig. 11(c) without the need for detection and post-processing. Such a real-time average could be particularly important where a clean pulse is needed directly in the optical domain.

D. Fractional Rep-Rate Division

Similar to Talbot-based rate multiplication concept, the Talbot-based rate division concept is also not limited to integer factors, but rather, it can be extended to realize repetition rate division and the associated amplification process of the original pulse train by any desired fractional factor. As shown in Fig. 4, a transition from the fractional distance of $z_T/3$ to the fractional distance of $z_T/2$ leads to repetition-rate division by a factor of $D = 3/2 = 1.5$. The rate division factor can be any desired fractional number, expressed as $D = m/p$, where m is the phase-modulation parameter, p is co-prime with m, and $m > p$. In this case, for example, for a phase modulation parameter of $m = 5$, the division factor will be $M = m/p = 5/p = 2.5, 1.66, 1.25$ (for $p = 2, 3, 4$, respectively). To implement the fractional rate division process in Fig. 5, the required temporal phase to be applied to the input pulses and the total dispersion required to achieve repetition rate division by the factor D are given by Eq. (5), φ_n, and following Eq. (8) [38], respectively.

$$\phi_2 = \beta_2 \Delta z_4 = (D-1)\, m \frac{T_{\text{in}}^2}{2\pi} \tag{8}$$

Fig. 12 shows the experimental validation of the concept of fractional repetition-rate division and corresponding Talbot amplification. Fig. 12(a) and (b) show the phase modulation functions, as prescribed by Eq. (5), for the phase modulation parameters of $m = 4$ and 5, respectively. Figs 12(c) and (d) show the temporal traces of the input and output trains for the rate division factors of $D = m/p = 4/3 = 1.33$ and $D = m/p = 5/2 = 2.5$. The original repetition rates of the input pulse trains in the two reported experiments are 7.9 GHz, and 18.8 GHz, and the reduced rates after the dispersion are 5.9 GHz, and 7.5 GH, respectively.

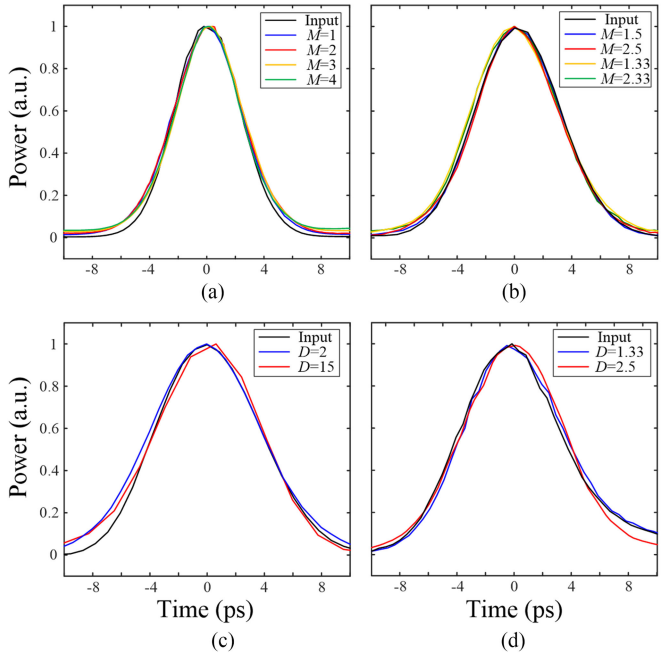

Fig. 13. Superposition of input and output individual pulse waveforms for (a) programmable integer rep-rate multiplication, (b) fractional rep-rate multiplication, (c) integer rep-rate division, and (d) fractional rep-rate division.

The central and perhaps most interesting result of the fractional repetition rate division, and associated fractional passive amplification, scheme is that it provides the possibility of achieving fractional averaging of the original repeating waveforms [38]. Such a capability is not defined by the mathematics of discrete averaging, which is strictly limited to application on an integer number of realizations of the process under test.

Finally, Fig. 13 shows the superposition of the pulse profile of the input and multiplied/divided output signals. As expected, in all cases, the output temporal pulses are nearly undistorted copies of the input pulses. The slight mismatch between input and output pulse shapes can be mainly attributed to the deviation of the actual dispersion value used in experiments from the ideal Talbot condition [34].

IV. Conclusion

In this paper, we have reviewed recent work on repetition-rate control of temporal pulse trains based on temporal Talbot effects. By manipulating both the temporal and spectral phase of an input pulse train according to temporal Talbot conditions, we can arbitrarily multiply and divide its repetition rate using a single device platform. Therefore, unlike previous work using the temporal Talbot effect, the desired rate multiplication or division factor need not be integer. Additionally, in the case of integer repetition-rate multiplication, the dispersive mechanism need not to be changed from one integer multiplication factor to the next. In this latest case, one need only to tune the temporal phase, which we show can be achieved at GHz speeds electronically through commercial fiber-integrated electro-optic phase modulators. Moreover, unlike traditional systems for repetition rate control, this method is energy-preserving, imparting

only insertion loss from the phase filtering devices. Additionally, because temporal Talbot effects coherently generate and delay frequency components, we observe and quantify noise mitigating effects of Talbot repetition rate manipulation, such as real-time optical averaging.

REFERENCES

[1] R. J. Essiambre, G. Kramer, P. J. Winzer, G. J. Foschini, and B. Goebel, "Capacity limits of optical fibre networks," *J. Lightw. Technol.*, vol. 28, no. 4, pp. 662–701, Feb. 2010.

[2] H. A. Haus and W. S. Wong, "Solitons in optical communications," *Rev. Mod. Phys.*, vol. 68, no. 2, pp. 423–444, Apr. 1996.

[3] F. Ferdous *et al.*, "Spectral line-by-line pulse shaping of on-chip microresonator frequency combs," *Nat. Photon.*, vol. 5, pp. 770–776, Mar. 2011.

[4] Z. Y. Zhang *et al.*, "1.55 mm InAs/GaAs quantum dots and high repetition-rate quantum dot SESAM mode-locked laser," *Sci. Rep.*, vol. 2, pp. 477-1–477-5, Jun. 2012.

[5] R. R. Gattass and E. Mazur, "Femtosecond laser micromachining in transparent materials," *Nat. Photon.*, vol. 2, pp. 219–225, Apr. 2008.

[6] S. A. Diddams, L. Hollberg, and V. Mbele, "Molecular fingerprinting with the resolved modes of a femtosecond laser frequency comb," *Nature*, vol. 445, pp. 627–630, Feb. 2007.

[7] D. R. Solli, C. Ropers, P. Koonath, and B. Jalali, "Optical rogue waves," *Nature*, vol. 450, pp. 1054–1057, Dec. 2007.

[8] P. Ghelfi *et al.*, "A fully photonics-based coherent radar system," *Nature*, vol. 507, pp. 341–345, Mar. 2014.

[9] R. Wang *et al.*, "Dissipative soliton in actively mode-locked fiber laser," *Opt. Express*, vol. 20, no. 6, pp. 6406–6411, Mar. 2012.

[10] L. N. Binh and N. Q. Ngo, *Ultra-Fast Fiber Lasers, Principles Applications With MATLAB Models*. Boca Raton, FL, USA: CRC Press, 2011.

[11] X. Yang, L. Zhang, H. Jiang, T. Fan, and Y. Feng, "Actively mode-locked Raman fiber laser," *Opt. Express*, vol. 23, no. 15, pp. 19831–19836, Jul. 2015.

[12] D. G. Revin, M. Hemingway, Y. Wang, J. W. Cockburn, and A. Belyanin, "Active mode locking of quantum cascade lasers in an external ring cavity," *Nat. Commun.*, vol. 7, May 2016, Art. no. 11440, doi: 10.1038/ncomms11440.

[13] Y. Zhou *et al.*, "Actively mode-locked all fiber laser with cylindrical vector beam output," *Opt. Lett.*, vol. 41, no. 3, pp. 548–550, Jan. 2016.

[14] A. Martinez and S. Yamashita, "Multi-gigahertz repetition rate passively modelocked fiber lasers using carbon nanotubes," *Opt. Express*, vol. 19, no. 7, pp. 6155–6163, Mar. 2011.

[15] L. Yang *et al.*, "A 110 GHz passive mode-locked fiber laser based on a nonlinear silicon-micro-ring-resonator," *Laser Phys. Lett.*, vol. 11, no. 6, Apr. 2014, Art. no. 065101.

[16] M. Peccianti *et al.*, "Demonstration of a stable ultrafast laser based on a nonlinear microcavity," *Nat. Commun.*, vol. 3, Apr. 2012, Art. no. 765, doi: 10.1038/ncomms1762.

[17] R. Paschotta, *Field Guide to Laser Pulse Generation*. Bellingham, WA, USA: SPIE, 2008.

[18] H. G. Weber and M. Nakazawa, *Ultrahigh-Speed Optical Transmission Technology*. Berlin, Germany: Springer, 2007.

[19] T. Papakyriakopoulos, K. Vlachos, A. Hatziefremidis, and H. Avramopoulos, "Optical clock repetition-rate multiplier for high-speed digital optical logic circuits," *Opt. Lett.*, vol. 24, no. 11, pp. 717–719, Jun. 1999.

[20] I. Ozdur, S. Ozharar, F. Quinlan, D. Mandridis, and P. J. Delfyett, "An interferometric method for high extinction ratio measurements with 60-dB dynamic range," *IEEE Photon. Technol. Lett.*, vol. 20, no. 24, pp. 2075–2077, Dec. 2008.

[21] K. Yiannopoulos *et al.*, "Rate multiplication by double-passing Fabry–Pérot filtering," *IEEE Photon. Technol. Lett.*, vol. 15, no. 9, pp. 1294–1296, Sep. 2003.

[22] H. Tsuda, Y. Tanaka, T. Shioda, and T. Kurokawa, "Analog and digital optical pulse synthesizers using arrayed-waveguide gratings for high-speed optical signal processing," *IEEE J. Lightw. Technol.*, vol. 26, no. 6, pp. 670–677, Mar. 2008.

[23] D. E. Leaird, A. M. Weiner, S. Kamei, M. Ishii, A. Sugita, and K. Okamoto, "Generation of flat-topped 500 GHz pulse bursts using loss engineered arrayed waveguide gratings," *IEEE Photon. Technol. Lett.*, vol. 14, no. 6, pp. 816–818, Jun. 2002.

[24] P. Petropoulos, M. Ibsen, M. N. Zervas, and D. J. Richardson, "Generation of a 40 GHz pulse stream by pulse multiplication with a sampled fiber Bragg grating," *Opt. Lett.*, vol. 25, no. 8, pp. 521–523, Apr. 2000.

[25] I. Kim, H. Sung, and D. Seo, "High-speed optical pulse train generation by line-by-line spectral intensity and phase coding," in *Proc. Int. Conf. Opto-Electron. Commun.*, 2012, pp. 919–920.

[26] A. Haboucha, W. Zhang, T. Li, M. Lours, A. N. Luiten, Y. Le Coq, and G. Santarelli "Optical-fiber pulse rate multiplier for ultralow phase-noise signal generation," *Opt. Lett.*, vol. 36, no. 18, pp. 3654–3656, Sep. 2011.

[27] D. Kielpinski and O. Gat "Phase-coherent repetition-rate multiplication of a mode-locked laser from 40 MHz to 1 GHz by injection locking," *Opt. Express*, vol. 20, no. 3, pp. 2717–2724, Jan. 2012.

[28] J. Magné *et al.*, "Generation of a 4×100 GHz pulse-train from a single-wavelength 10-GHz mode-locked laser using superimposed fiber bragg gratings and nonlinear conversion," *IEEE J. Lightw. Technol.*, vol. 24, no. 5, pp. 2091–2099, May 2006.

[29] J. Azaña and M. A. Muriel, "Temporal self-imaging effects: Theory and application for multiplying pulse repetition-rate s," *IEEE J. Sel. Topics Quant. Electron.*, vol. 7, no. 4, pp. 728–744, Jul. 2001.

[30] G. Meloni, G. Berrettini, M. Scaffardi, and A. Bogoni, "250-times repetition frequency multiplication for 2.5 THz clock signal generation," *IEEE Electron. Lett.*, vol. 41, no. 23, pp. 1294–1295, Nov. 2005.

[31] J. H. Lee *et al.*, "$2 \sim 5$ times tunable repetition-rate multiplication of a 10 GHz pulse source using a linearly tunable, chirped fiber Bragg grating," *Opt. Express*, vol. 12, no. 17, pp. 3900–3905, Aug. 2004.

[32] S. Atkins, D. Dahan, and B. Fischer, "All-optical pulse-rate multiplication using fractional Talbot effect and field to intensity conversion by cross gain modulation," *IEEE Photon. Technol. Lett.*, vol. 15, no. 1, pp. 132–134, Jan. 2003.

[33] D. Pudo and L. R. Chen, "Simple estimation of pulse amplitude noise and timing jitter evolution through the temporal Talbot effect," *Opt. Express*, vol. 15, no. 10, pp. 6351–6357, May 2007.

[34] R. Maram, L. Romero Cortés, and J. Azaña, "Programmable fiber-optics pulse repetition-rate multiplier," *IEEE, J. Lightw. Technol.*, vol. 34, no. 1, pp. 5403–5406, Jan. 2016.

[35] R. Maram, J. Van Howe, M. Li, and J. Azaña, "Lossless fractional pulse repetition-rate multiplication of optical pulse trains," *Opt. Lett.*, vol. 40, no. 3, pp. 375–378, Feb. 2015.

[36] R. Maram, J. Van Howe, M. Li, and J. Azaña, "Noiseless intensity amplification of repetitive signals by coherent addition using the temporal Talbot effect," *Nat. Commun.*, vol. 5, pp. 4827, Oct. 2014, doi:10.1038/ncomms6163.

[37] R. Maram, J. Van Howe, and J. Azaña, "Demonstration of input-to-output gain in a Talbot amplifier," in *Proc. IEEE Int. Conf. Photon.*, 2015, Reston, VA, USA, Paper: TuB2.5.

[38] L. Romero Cortés, R. Maram, and J. Azaña, "Fractional averaging of repetitive waveforms induced by self-imaging effects," *Phys. Rev. A*, vol. 92 no. 4, Oct. 2015, Art. no. 041804.

[39] H. Guillet de Chatellus, E. Lacot, O. Hugon, O. Jacquin, N. Khebbache, and J. Azaña "Phases of Talbot patterns in angular self-imaging," *J. Opt. Soc. Amer. A*, vol. 32, no. 6, pp. 1132–1139, Jun. 2015.

[40] L. R. Cortés, H. G. d. Chatellus, and J. Azaña, "On the generality of the Talbot condition for inducing self-imaging effects on periodic objects," *Opt. Lett.*, vol. 41, no. 2, pp. 340–343, Jan. 2016.

[41] J. Caraquitena, M. Beltrán, R. Llorente, J. Martí, and M. A. Muriel, "Spectral self-imaging effect by time-domain multilevel phase modulation of a periodic pulse train," *Opt. Lett.*, vol. 36, no. 6, pp. 858–860, Mar. 2011.

[42] A. Malacarne and J. Azaña, "Discretely tunable comb spacing of a frequency comb by multilevel phase modulation of a periodic pulse train," *Opt. Express*, vol. 21, no. 4, pp. 4139–4144, Feb. 2013.

[43] Reza Salem, A. Mark . Foster, and L. Alexander Gaeta, "Application of space–time duality to ultrahigh-speed optical signal processing," *Adv. Opt. Photon.*, vol. 5, pp. 274–317, Aug. 2013.

[44] R. Maram and J. Azaña, "Spectral self-imaging of time-periodic coherent frequency combs by parabolic cross-phase modulation," *Opt. Express*, vol. 21, no.23, pp. 28824–28835, Nov. 2013.

[45] L. Lei *et al.*, "Observation of spectral self-imaging induced on a frequency comb by nonlinear parabolic cross-phase modulation," *Opt. Lett.*, vol. 40, no. 22, pp. 5403–5406, Nov. 2015.

[46] R. Maram, J. Van Howe, and J. Azaña, "Noise-eating amplifier for repetitive signals," in *Proc. IEEE Photon. Conf.* , 2014, San Diego, CA, USA, Paper: WE2.2.

[47] J. Azaña, R. Maram, J. Van Howe, and M. Li, "Passive amplification and real-time averaging of repetitive waveforms by Talbot effect," in *Proc. Eur. Conf. Lasers Electro-Opt.*, 2015, Paper: CI-4.1.

Reza Maram received the M.Sc. degrees in optoelectronics engineering from the University of Tabriz, Tabriz, Iran, in 2009. From 2007 to 2011, he was working as a Researcher in the Photonic and Nanocrystal Research Laboraoty, University of Tabriz under the supervision of Prof. Ali Rostami. In 2012, he joined the Ultrafast Optical Processing Group, INRS-EMT as a Ph.D. student, working under the supervision of Prof. José Azaña, and accomplished the Ph.D. studies in November 2016. Since then, he has been a Postdoctoral Research Fellow at the same group at INRS-EMT.

He has to his credit above 40 publications in top scientific journals and technical conferences, including 14 contributions in high-impact peer-review journals (IOP, IEEE, OSA, and Nature editorial groups) and one text book in Springer. His recent research interests include optical self-imaging, ultrafast all-optical information processing and computing, energy efficiency photonics, and nonlinear optic.

Mr. Maram is a Student Member of the Optical Society of America. He received the doctoral scholarship for foreign students from the Québec Government, Canada.

Luis Romero Cortés was born in Huelva, Spain, on December 14, 1988. He received the B.Sc. degree (five-year program) in telecommunications engineering and the M.Sc. degree in electronic systems, signal processing, and communications from the Universidad de Sevilla, Sevilla, Spain, in 2011 and 2012, respectively. He is currently working toward the Ph.D. degree with the Ultrafast Optical Processing Group, Institut National de la Recherche Scientifique–Energie, Matériaux et Télécommunications, Université du Québec, Montréal, Canada, working under the supervision of Prof. José Azaña. During the course of the B.Sc. studies, he worked at the Instituto de Óptica of the Spanish High Research Council, in Madrid, Spain, under the supervision of Dr. Juan Diego Ania Castañón, in the field of nonlinear optics, and received a national scholarship which he dedicated to work in the fields of advanced modulation formats in coherent optical communication systems and spectral interferometry techniques for optical signal characterization with Prof. Alejandro Carballar Rincón. During the course of the M.Sc. studies, he worked at the Center of Advanced Aerospace Technologies, Sevilla, Spain, in the field of space-time signal processing for unmanned aerial vehicle communication systems.

His recent research interests include the study of self-imaging effects in multiple domains, optical frequency combs, and ultrafast optical signal processing.

Mr. Cortés is a student member of the Optical Society of America and the International Society for Optics and Photonics.

James Van Howe received the B.A. degree in physics from the University of Chicago, Chicago, IL, USA, in 2001, and the M.S. and Ph.D. degrees in physics from Cornell University, Ithaca, NY, USA, in 2005 and 2007, respectively. His current research interests include ultrafast optical signal processing, nonlinear optics, space-time analogs in optical systems, and quantum optical processing. He has authored or coauthored more than 30 journal articles and conference proceedings and has three patents on his work. He is an Associate Professor and the current department Chair of the Department of Physics and Astronomy, Augustana College, Rock Island, IL, USA. He was a Visiting Professor at Institut National de la Recherche Scientifique–Centre Energie, Matériaux et Télécommunications, Montreal, QC, Canada during the summers of 2012 and 2016. He is a member of the Optical Society of America.

José Azaña received the Telecommunication Engineer degree and the Ph.D. degree in Telecommunication Engineering from the Universidad Politécnica de Madrid, Madrid, Spain. He is currently a Professor and a Canada Research Chair at the Institut National de la Recherche Scientifique–Centre Energie, Matériaux et Télécommunications, Montreal, QC, Canada.

His research interests include ultrafast photonics, optical signal processing, all-fiber and integrated-waveguide technologies, high-speed telecommunications, all-optical computing, measurement of ultrafast events, light pulse interferometry, and broadband microwave signal generation and manipulation. He has to his credit about 450 publications in top scientific journals and technical conferences, including more than 200 contributions in high-impact peer-review journals (with most publications in the IEEE, OSA, and Nature Editorial Groups), and many invited and coinvited journal publications and presentations in leading international meetings.

Prof. Azaña is a Fellow of the Optical Society of America and his research work has been recognized with several prestigious awards and distinctions at institutional, national, and international levels, including the 2008 IEEE-Photonics Society Young Investigator Award, and the 2009 IEEE-MTT Society Microwave Prize.